Eur. Phys. J. A **10**, 259–265 (2001)

THE EUROPEAN PHYSICAL JOURNAL A

High-spin states in ^{208}Pb

J. Wrzesiński[1,a], K.H. Maier[1,2], R. Broda[1], B. Fornal[1], W. Królas[1], T. Pawłat[1], D. Bazzacco[3], S. Lunardi[3], C. Rossi Alvarez[3], G. de Angelis[4], A. Gadea[4], J. Gerl[5], and M. Rejmund[6]

[1] Niewodniczański Institute of Nuclear Physics, PL-31-342 Kraków, Poland
[2] Hahn-Meitner Institut, D-14109 Berlin, Germany
[3] Dipartimento di Fisica dell'Università and INFN Sezione di Padova, I-35131 Padova, Italy
[4] INFN Laboratori Nazionali di Legnaro, I-35020 Legnaro, Italy
[5] Gesellschaft für Schwerionenforschung, Darmstadt, Germany
[6] DAPNIA/SPhN, CEA Saclay, F91191 Gif-sur Yvette Cedex, France

Received: 31 October 2000
Communicated by D. Schwalm

Abstract. High-spin states in ^{208}Pb have been studied by γ-ray-spectroscopy methods in deep inelastic reactions induced by beams of ^{208}Pb, ^{136}Xe and ^{76}Ge beams on a thick ^{208}Pb target. The 11_2^+ state and new γ-transitions between the one-particle one-hole states of highest spin have been found and electromagnetic matrix elements verified. High-spin states of two-particle two-hole structure have been detected for the first time. The results are compared to shell model calculations with realistic interactions in the complete Kuo-Herling space.

PACS. 21.60.Cs Shell model – 23.20.Lv Gamma transitions and level energies – 27.80.+w $190 \leq A \leq 219$ – 25.70.Lm Strongly damped collisions

1 Introduction

The study of excited states in ^{208}Pb, as the heaviest doubly magic nucleus, offers unique possibilities for a basic understanding of the single-particle structure of the nucleus. Kuo and Herling [1] derived already in 1970 the residual interaction between nucleons occupying the shell model orbitals around ^{208}Pb from the interaction between free nucleons. This interaction was used quite successfully, as shown for instance by Warburton and Brown [2]. Usually, in these calculations the single-particle energies are taken from the experimental energies of appropriate levels in nuclei with one particle or hole. But there is now also a phenomenological potential, that reproduces the single-particle energies quite well [3]. The theoretical efforts continue; very recently Coraggio *et al.* [4] determined the residual interaction between proton particles around ^{208}Pb from the Bonn potential for free nucleons. Their calculations are similar to those performed by Kuo and Herling, but have now been done without previously necessary computational simplifications. The interaction, that they derived, reproduces the level energies of the two-proton nucleus ^{210}Po even better than the Kuo Herling interaction [1] with the adjustments by Warburton and Brown [2]. Similar calculations were done for most of the other subspaces, in particular for neutron holes (see refs. given in [4]), but keeping ^{208}Pb as an inert core, *i.e.* excluding particle-hole excitations. Recently A. Brown [5] calculated a realistic interaction from the H7B interaction [6] for the complete Kuo-Herling space; this space has $^{132}_{50}$Sn$_{82}$ as inert core and comprises the orbitals, that would be filled for the nucleus $^{310}_{126}$X$_{184}$. These calculations included in particular also the interaction between the orbitals below and above the shell closure in ^{208}Pb, that are needed to describe the excited particle-hole states in ^{208}Pb itself. Another important development has occurred with shell model computations, *i.e.* calculating nuclear properties from a given interaction. Many more active particles and a larger configuration space can now be treated. Consequently, many more nuclear states are now accessible for detailed shell model calculations. Of direct relevance for this work is, that it has become possible to calculate two-particle two-hole states in ^{208}Pb for the complete Kuo-Herling space with the OXBASH code.

Experimental data on γ-transitions and high-spin states in ^{208}Pb are still scarce, because ^{208}Pb is too neutron rich for the usual studies with fusion-evaporation reactions. However, γ-spectroscopy following deep inelastic reactions has made it possible to find new states at higher spins and the γ-transitions between them [7,8]. Schramm

[a] e-mail: Jacek.Wrzesinski@ifj.edu.pl

et al. [9] found the main γ-cascade from the one-particle one-hole state with the highest spin 14^- by inelastic scattering of ^{64}Ni and ^{82}Se on ^{208}Pb. The experiments, presented here, used heavier beams on ^{208}Pb targets and found with more efficient detector systems new levels and transitions. Parts of the present results have been preliminarily reported already at earlier conferences [10,11]. In this article the advances of theory are compared and tested with the new experimental results.

2 Experiments

In an earlier experiment, performed at the INFN Legnaro, the 420 MeV ^{76}Ge beam from the ALPI linear accelerator bombarded a thick (50 mg/cm^2) ^{208}Pb target, placed in the center of the GASP Ge-detector array. The very low beam intensity of around 0.2 pnA, available at that time, limited the statistics of the collected coincidence data. On the other hand, the beam pulsing with 400 ns repetition time and the low intensity provided a very clean identification of the γ-rays preceding the 10^+ isomer ($T_{1/2} = 500$ ns) by prompt delayed coincidences.

In two later experiments at the UNILAC of GSI, Darmstadt, a thick ^{208}Pb target was hit by beams of 5.7 MeV/u ^{136}Xe and 6.5 MeV/u ^{208}Pb and γ-rays were detected by 5 Ge-CLUSTER detectors of the EUROBALL project [12] placed in a ring close to 180° and 132 NaI scintillators of the CRYSTAL BALL [13]. This set-up has already been described together with the data on ^{209}Pb and ^{210}Pb [14,15]. The beam was pulsed with 110 ns distance between pulses. These experiments provided better statistics on prompt-prompt coincidences. The data from all three experiments were used, to deduce the final results.

3 Results

Figure 1a shows the spectrum of prompt γ-rays in coincidence with delayed γ-transitions occurring in the decay of the 10^+ isomer, as measured with the ^{76}Ge beam and the GASP spectrometer. All lines, that are placed into the level scheme (fig. 2) above the 10^+ isomer are indicated. Table 1 lists the energies and intensities as derived from this spectrum and also the prompt γ-intensities which were obtained from a best fit of the prompt-prompt coincidences of the experiment with the ^{208}Pb beam and the cluster detectors. This fit was performed for the level scheme of fig. 2 with the program ESCAL8R as described in ref. [16]. The intensities from both experiments agree surprisingly well. Apparently the feeding pattern is not very different for the various beams used, and the impact of the angular distribution of γ-rays is not important, although the detector arrangement of GASP is isotropic, while the cluster detectors were all placed close to 180°. The highest-lying transitions at 290.7 and 947.6 keV are suppressed in the Pb-data by the prompt time window, because they are partly fed from a higher-lying isomer.

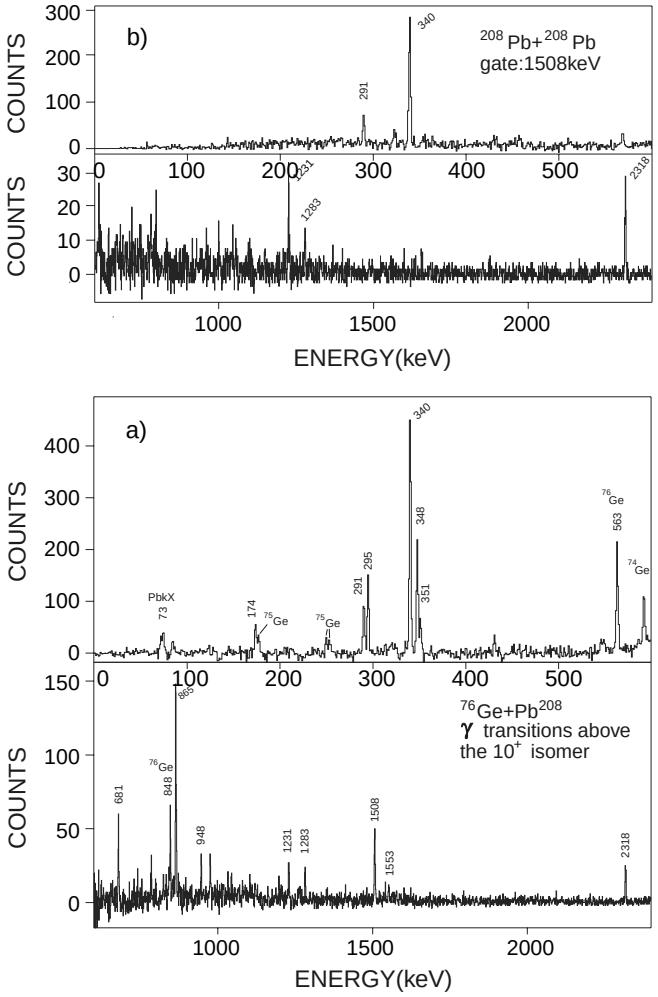

Fig. 1. a) Spectrum of prompt and short delayed γ-rays in coincidence with lines below the 10^+ isomer, 284, 583, 1412 and 2614 keV. b) Spectrum in prompt-prompt coincidence with the 1508 keV line from the experiment with the ^{208}Pb beam. A "banana" gate has been used for the coincidence time that is narrow at high energies and wider for low energies; therefore the 948 keV line is not evident.

The previously known lines [9] below the 14^- state are evident and confirm the known yrast scheme between the 10^+ and 14^- states. The 1508 and 1553 keV lines are new; they are $E3$ crossover transitions from 14^- to 11^+ and 13^- to 10^+ states, as proven by coincidence relationships and their matching energies. The spectrum in coincidence with the 1508 keV line (fig. 1b) shows the preceding lines above the 14^- level and the following 340 keV transition to the 10^+ isomer.

A new γ-cascade of 351 and 681 keV proceeds from the 12^+ level to the second 10^+ state through a new state at 5749 keV. The selection rules for the connecting γ-transitions limit its spin to 10, 11, or 12. There are very few one-particle one-hole configurations, that can give these spins around this energy. The four expected 10^+ states and the one 12^+ level are known already,

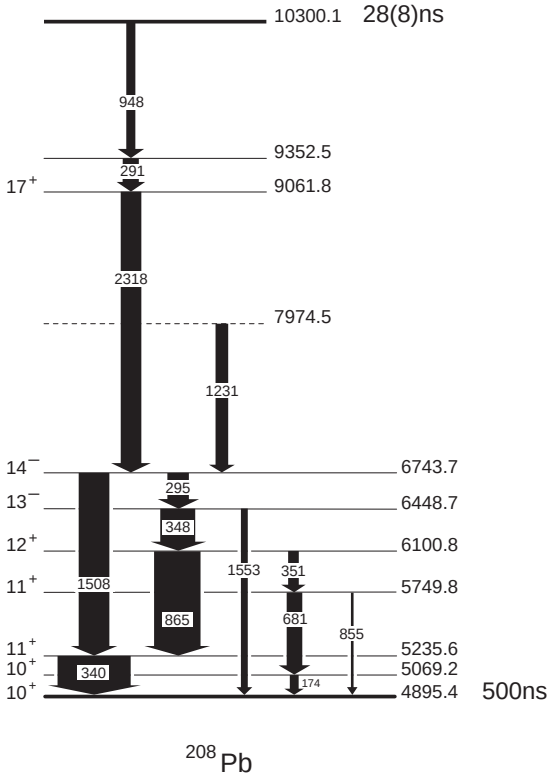

Fig. 2. Levels and γ-transitions in ^{208}Pb above the 10^+ isomer from the present experiments. The level energies have errors of 0.2 keV at the bottom, rising to 0.5 keV. The width of the arrows reflects the γ-intensities as in column 3 of table 1.

Table 1. Gamma-ray transitions assigned to ^{208}Pb above the 10^+ isomer.

	^{208}Pb+^{208}Pb	^{76}Ge+^{208}Pb
$E_\gamma(keV)$[a]	I_γ[b]	I_γ[d]
173.9	7 (2)	12 (2)
290.7	12 (1)	22 (2)
295.3	20 (2)	28 (3)
340.2	100 (5)[c]	100 (6)
347.9	51 (3)	48 (4)
351.4	11 (2)	15 (2)
680.6	19 (6)	21 (4)
854.6	-	3 (2)
865.2	55 (4)	64 (13)[e]
947.6	2 (1)	12 (3)
1230.8	16 (2)	17 (2)
1283.4	-[f]	12 (2)
1508.1	45 (3)	42 (7)
1552.7	7 (2)	10 (4)
2318.1	24 (2)	28 (4)

a) Typical uncertainties on the γ-ray energies are 0.2 keV.

b) Intensities fitted with ESCAL8R program [16] on prompt coincidence γ-γ matrix. Indicated errors are from program estimates and do not include angular distribution and correlation effects.

c) Intensity sum of the feeding transitions 1508 keV and 865 keV.

d) Intensities deduced from the sum coincidence spectrum with delayed transitions below the 10^+ isomer: 284 keV, 583 keV, 1413 keV and 2614 keV. Time windows: prompt $-25\,\mathrm{ns} < t < 30\,\mathrm{ns}$, delayed $30\,\mathrm{ns} < t < 600\,\mathrm{ns}$ with the region around the next prompt peak excluded. The errors are statistical only.

e) Doublet, cross-coincidence with transition in ^{74}Ge.

f) Weakly observed in ^{208}Pb+^{208}Pb experiment; not placed in level scheme.

and negative-parity states are not expected at all. This leaves only the 11^+ level of the configuration $\nu i_{11/2} i_{13/2}^{-1}$, and this assignment agrees perfectly with all observed γ-transitions. The shell model predictions are so clear in this case, that 11^+ can be assigned to the 5749 keV state. A second, weak decay branch from this level to the lowest 10^+ level is also observed.

The strongest transition above the 14^- state is the 2318 keV line. As discussed in ref. [17] it can be assigned as the collective octupole excitation built on top of the $(\nu j_{15/2} i_{13/2}^{-1}; 14^-)$ state and coupled to a maximum spin 17^+. The energy agrees very well with the combined shifts of the observed particle-octupole couplings of the individual $\nu j_{15/2}$ and $i_{13/2}^{-1}$ orbitals [17]. A cascade of 948 and 291 keV lines populates the 9062 keV level. The ordering of both transitions is clear and both show a delayed component with the time distribution as presented in fig. 3. A half-life of $T_{1/2} = 28(8)$ ns is deduced for this higher-lying isomer. The scarce statistics cannot rule out, that the 948 keV line has a prompt component and the isomeric transition has been missed. On the other hand, an $E3$ multipolarity of the 948 keV transition with strength as found for the other $E3$ transitions would match the lifetime well. A line at 1230.8 keV is definitely located above the 14^- state and probably also a 1283.4 keV line; both most likely populate the 14^- level directly.

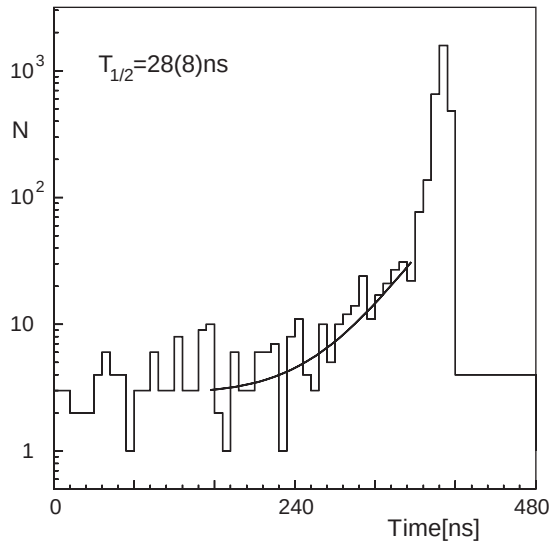

Fig. 3. Summed intensity of the 291, 295, 340, 348, 865, 948, 1508 and 2318 keV transitions relative to the pulsed beam, showing the half life of the new high-spin isomer in ^{208}Pb. The best fit of an exponential plus constant background, that gives $T_{1/2} = 28(8)$ ns, is also shown.

4 Discussion

4.1 One-particle one-hole states

High-spin states in ^{208}Pb have been studied previously in inelastic electron and proton scattering [18–20]. The assignments of these very different experiments agree for the 10^+, 12^+, and 14^- levels with the present findings. They also found a 12^- level very close to our 13^- level [18, 19]; later this 12^- level has been shown to be a doublet with likely a 13^- state in inelastic proton scattering [21], that then has to be identical with the level seen here. However, the second 11^+ level was placed at 5.860 MeV from electron scattering data [20] in disagreement with the present work. There is also disagreement for the first 11^+ state [9]. Neutron states are weakly excited in inelastic electron scattering, and even at the achieved resolution of 20 keV unresolved multiplets pose big problems.

The structure of the one-particle one-hole states in general has been discussed by Rejmund *et al.* [22]. For the high-spin states, only one configuration gives negative parity, namely $\nu j_{15/2} i_{13/2}^{-1}$ that extends to 14^-, which is the highest possible spin from any one-particle one-hole configuration. The configuration $\nu i_{11/2} i_{13/2}^{-1}$ reaches to maximum spin 12^+, $\nu g_{9/2} i_{13/2}^{-1}$ to 11^+, and for spin 10^+ the configurations $\nu j_{15/2} f_{5/2}^{-1}$ and $\pi h_{9/2} h_{11/2}^{-1}$ are also possible. The four known [23] 10^+ levels show a pronounced mixing of these four configurations [22]. On the other hand, the two 11^+ states do not show any mixing of the two possible configurations (see below), and for spins from 12 to 14 anyway only one configuration is possible.

As the structure of the levels is so pure and well known, their γ-decay can be interpreted in detail. In the decay of the 14^- level the new $E3$ transition to the 11_1^+ state competes with the $M1$ transition to 13^- state. This is exceptional. The $B(E3)$-value of the transition from $(j_{15/2} i_{13/2}^{-1}; 14^-)$ to $(g_{9/2} i_{13/2}^{-1}; 11^+)$ is for this stretched coupling the same as $B(E3, j_{15/2} \rightarrow g_{9/2})$ for the single particles. It has been measured in ^{209}Pb as $B(E3, j_{15/2} \rightarrow g_{9/2}) = 25^{+7}_{-4}$ W. u. [24]. This gives a decay rate $\lambda(14^- \rightarrow 11^+) = 0.64 \cdot 10^9\,\mathrm{s}^{-1}$ with limits of 0.54 and $0.83 \cdot 10^9\,\mathrm{s}^{-1}$. The measured branching ratio $I(295\ \mathrm{keV})/I(1508\ \mathrm{keV}) = 0.67(13)$ means then $\lambda(14^- \rightarrow 13^-) = 0.43(15) \cdot 10^9\,\mathrm{s}^{-1}$. This is very slow for the possible $M1$ transition, corresponding to $B(M1) \leq 10^{-3}$ W. u. Indeed, one also calculates a very small $B(M1, (j_{15/2} i_{13/2}^{-1}; 14^-) \rightarrow (j_{15/2} i_{13/2}^{-1}; 13^-))$ for pure configurations and the adopted [22] single-particle magnetic moments; the $M1$ transition strength is proportional to $(g(j_{15/2}) - g(i_{13/2}^{-1}))^2$ and the g-factors are nearly equal. As these decays are so slow, other usually negligible modes have also to be considered. One of them is the $M2$-decay to the $(\nu i_{11/2} \nu i_{13/2}^{-1}; 12^+)$ state. This is analogous to the $M2$ branch from $\nu j_{15/2}$ to $\nu i_{11/2}$ in ^{209}Pb, that proceeds with 12% of the $E3$-transition to $\nu g_{9/2}$ [15,24]. The transition strengths should be identical for the states in ^{208}Pb, with just an $i_{13/2}$ neutron hole coupled to these neutrons with maximum spin. The $(14^- \rightarrow 12^+)$ transition in ^{208}Pb with a calculated energy of 643 keV is then expected with 8% of the 1508 keV line, well below the detection limit of the present experiment. Next, $E2$ transitions, that are usually negligible in ^{208}Pb compared with $M1$ transitions, have also to be considered. The $(\,(j_{15/2} i_{13/2}^{-1}; 14^-) \rightarrow (j_{15/2} i_{13/2}^{-1}; 12^-)\,)$ $E2$ transition is calculated to be 4 orders of magnitude weaker, and it remains negligible, if one varies $\langle j_{15/2} \,||\, M(E2) \,||\, j_{15/2} \rangle = -64\,\mathrm{efm}^2$, that is only known [22] from theory; the 12^- level is known at 6.43 MeV [21] from $(\mathrm{p}, \mathrm{p}')$. But, surprisingly, the transition rate of the $(\,(j_{15/2} i_{13/2}^{-1}; 14^-) \rightarrow (j_{15/2} i_{13/2}^{-1}; 13^-)\,)$ $E2$ transition with $\Delta I = 1$ is calculated as $\lambda = 0.38 \cdot 10^9\,\mathrm{s}^{-1}$, which is very similar to the $M1$ and $E3$ rates.

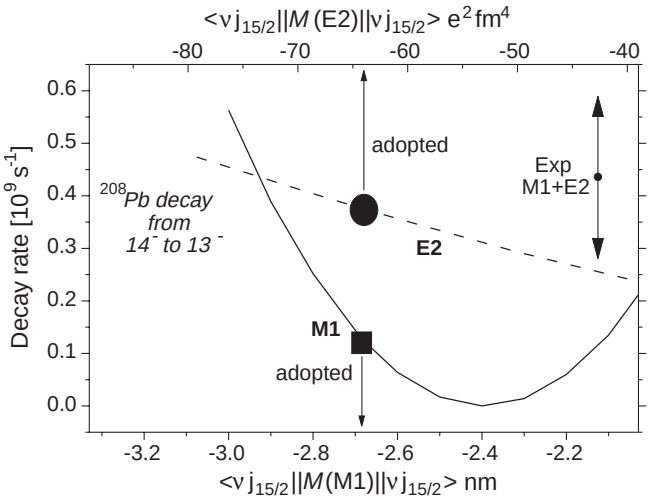

Fig. 4. Decay from the 14^- to the 13^- state. The total $14^- \rightarrow 13^-$ decay rate, determined from the measured branching ratio and the $\nu j_{15/2} \rightarrow \nu g_{9/2}$ transition rate in ^{209}Pb is shown. It is compared with the theoretical $M1$- and $E2$- decay rates as a function of the $\nu j_{15/2}$ matrix elements (top and bottom scale). The adopted values are indicated; their sum agrees with the measurement.

The $M1$- and $E2$-matrix elements of the $i_{13/2}$ neutron hole are precisely measured, but those of the $j_{15/2}$ neutron are only known from theory [25,26]. Therefore fig. 4 shows the calculated $M1$- and $E2$- decay rates as a function of $\langle j_{15/2} \,||\, M(M1) \,||\, j_{15/2} \rangle$ and $\langle j_{15/2} \,||\, M(E2) \,||\, j_{15/2} \rangle$ around their adopted values. The total (sum of $M1$ and $E2$) $(14^- \rightarrow 13^-)$ decay rate as determined from the experiment (see above) is also shown. The sum of the calculated $M1$- and $E2$-rates agrees with the measurement. It is seen that the $E2$-decay dominates and might even exhaust the full transition strength and that it depends only weakly on the single-particle matrix element. A perfect cancellation of the $M1$-transition amplitudes due to the $i_{13/2}$-neutron hole and the $j_{15/2}$-neutron occurs for $\langle j_{15/2} \,||\, M(M1) \,||\, j_{15/2} \rangle = -2.4\,\mathrm{nm}$ close to the adopted value of $-2.68\,\mathrm{nm}$. The consistence of the measured branching ratio with the calculated decay rates proves that the wave functions are very pure and that the

adopted matrix elements are right. It is not trivial, that the allowed $M1$- and $E2$-decays are both so weak.

The $E3$ crossover transition from the 13^- level to the lowest 10^+ with 1553 keV is again a $\nu j_{15/2} \rightarrow \nu g_{9/2}$ transition. Its $B(E3)$-value is calculated as 50 % of that in ^{209}Pb (the probability of the populated $\nu g_{9/2} i_{13/2}^{-1}$ configuration in the 10+ state is 0.62 and angular momentum coupling for this nonstretched transition reduces the $B(E3)$ by additional factor of 0.75) resulting in a rate of 0.5 10^9 s^{-1}. The main $E1$ branch, 348 keV from 13^- to 12^+ state is then hindered by about 10^6.

The γ-decay of the new 11_2^+ state can be used to check the wave functions of the 10^+ and 11^+ states and the $M1$ matrix elements involving the $i_{11/2}$ neutron, that are only known from theory [25,26]. The branching from 11_2^+ to the two lowest 10^+ levels agrees within errors with the calculated ratio for the empirical wave functions of ref. [22]. The calculated total decay rate [22] of $2 \cdot 10^{11}\,\mathrm{s}^{-1}$ and the now measured limit of 5% for the decay to the lower 11^+ level restrict the configuration mixing between the two 11^+ states. The wave function of the upper 11^+ state shall be expressed as $\sqrt{1-a^2} \cdot \nu i_{11/2} i_{13/2}^{-1} + a \cdot \nu g_{9/2} i_{13/2}^{-1}$ and that of the lower one as orthogonal to this. Then $-0.05 \leq a \leq +0.1$ is deduced, or $a^2 \leq 0.01$. Because the $M1$ elements $\langle i_{11/2} \,||\, M(M1) \,||\, g_{9/2} \rangle$ and $\langle i_{11/2} \,||\, M(M1) \,||\, i_{11/2} \rangle$ are not so certain, this limit might be somewhat higher. But $a^2 \leq 0.03$ is a safe estimate. The transition rate is very sensitive to the mixing; for pure configurations only the small, l-forbidden element $\langle \nu i_{11/2} \,||\, M(M1) \,||\, \nu g_{9/2} \rangle = 0.35\,\mathrm{nm}$ contributes, while the mixing between the two configurations allows the transition to proceed with the strong element $\langle \nu g_{9/2} i_{13/2}^{-1}; 11^+ \,||\, M(M1) \,||\, \nu g_{9/2} i_{13/2}^{-1}; 11^+ \rangle = -5.91\,\mathrm{nm}$. The branching from the 11_2^+ state to the two lowest 10^+ levels depends primarily on the value of the $M1$ matrix element involving the $i_{11/2}$ neutron orbital and the amplitudes of the $\nu i_{11/2} i_{13/2}^{-1}$ configuration in the 10^+ states. Therefore these quantities, as presented in ref. [22], are confirmed.

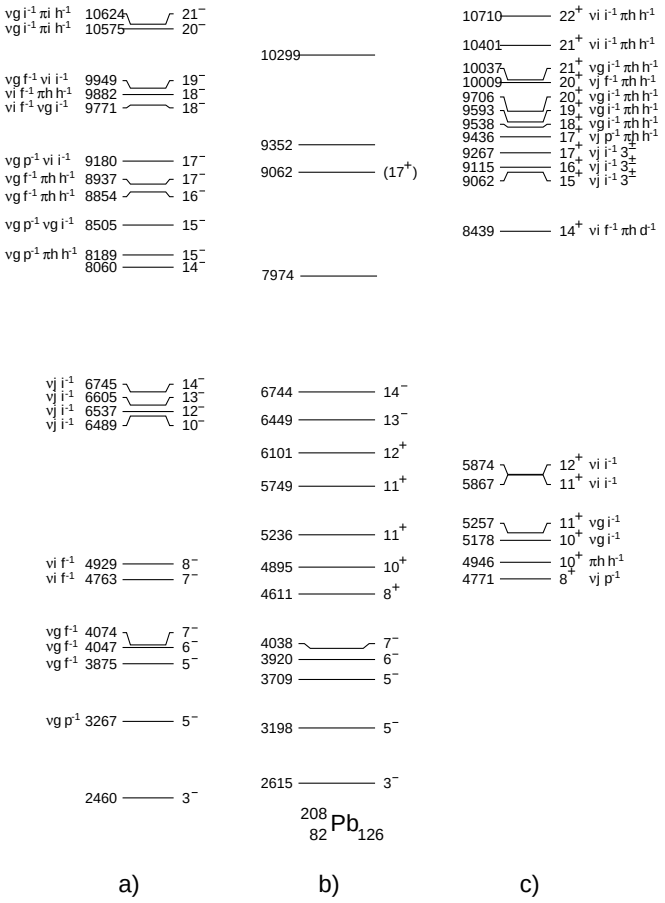

Fig. 5. Comparison of the experimental b) level scheme of ^{208}Pb with the results of shell-model calculations. Column a) shows the negative- and c) the positive-parity states. The leading configuration of the state is also given. The following shorthand notation is used for the configurations: (π) $h \equiv 1h_{9/2}$, $i \equiv 1i_{13/2}$, $h^{-1} \equiv 1h_{11/2}^{-1}$ and neutrons (ν) $g \equiv 2g_{9/2}$, $i \equiv 1i_{11/2}$, $j \equiv 1j_{15/2}$, $p^{-1} \equiv 3p_{1/2}^{-1}$, $f^{-1} \equiv 2f_{5/2}^{-1}$, $i^{-1} \equiv 1i_{13/2}^{-1}$. All energies are given in keV.

4.2 Two-particle two-hole states

Full scale shell model calculations are required to gain an overview of the possible two-particle two-hole states close to the yrast line. OXBASH calculations have been made possible by Alex Brown [5] for the full "Kuo-Herling space". This space has $^{132}_{50}$Sn$_{82}$ as core and extends to $^{310}_{126}$X$_{184}$. It includes, relative to ^{208}Pb as core, 5 proton hole, 6 neutron hole, 6 proton particle and 7 neutron particle orbitals. The single-particle energies of these orbitals have been taken from experiment (see fig. 1 of ref. [22]). This is the usual choice with the Kuo-Herling interaction [2]. Calculations of the two-particle two-hole states in ^{208}Pb require the complete set of matrix elements between any particle and hole orbitals. Particle-particle and hole-hole interactions have been calculated by Kuo and Herling [1] and then checked and adjusted. We used the particle-particle interaction of Warburton and Brown [2] for the orbitals above ^{208}Pb. For the orbitals below (the holes) the two-body matrix elements of Kuo and Herling [1], as adjusted and given by Rydström, and Blomqvist *et al.* [27], have been used for the proton-proton and proton-neutron multiplets. The neutron-neutron interaction was taken from McGrory and Kuo [28]. Kuo and Herling did not calculate the interaction between orbitals above and orbitals below the shell gaps at ^{208}Pb. These matrix elements have now been calculated by B.A. Brown [5] according to the procedure of Kuo and Brown [29] from the H7B free nucleon potential [6]. This part of the interaction has not yet been adjusted to experimental data. The relevant part of the level scheme, calculated with this interaction by the OXBASH code, is compared with experiment in fig. 5.

If the 1230.8 and the less certain 1283.4 keV transitions really populate the 14^- level directly, they can be assigned to the theoretical 14^- and 15^- states, as no oth-

ers are calculated close enough. The structure of these states is mainly of the $(10^+ \otimes \nu g_{9/2} p_{1/2}^{-1})$ configuration. The 9062 keV level is the octupole vibration on top of the 14^- state as discussed in ref. [17]. The shell model calculation predicts this state 200 keV higher, although the 3^- state itself is calculated 150 keV too low. The transitions above the 17^+ level cannot be assigned to calculated states, the density of calculated states in fig. 5 being too high. An inspection of fig. 5 does not show any obvious candidate for an isomer either. The realistic interaction reproduces the well-known one-particle one-hole states remarkably well. There are however deviations up to 200 keV. This shows the need to adjust the interaction, as it has been done for the other subspaces. Predictions for the two-particle two-hole states should then be much more meaningful. But, although calculations with an adjusted interaction might help, an experimental determination of spins and multipolarities is needed.

5 Conclusions

The newly found 11_2^+ state and its γ-decay agree fully with the theoretically expected properties. This verifies the structure [22] of the two 11^+ and the lowest two 10^+ states, that are involved, and confirms the calculated values of the $M1$ matrix elements $\langle i_{11/2} \mid\mid M(M1) \mid\mid i_{11/2} \rangle$ and $\langle i_{11/2} \mid\mid M(M1) \mid\mid g_{9/2} \rangle$. The, at first sight, highly surprising branching from the 14^- level agrees perfectly with detailed calculations and confirms the electromagnetic matrix elements used in ref. [22] for the $j_{15/2}$ neutron. Any additional information on the 14^- state decay, as the $M1/E2$ mixing of the 295 keV line, would provide further evidence on the electromagnetic matrix elements. The study of the $M1$- and $E2$-properties of the single-particle orbitals, which deviate much from the values expected in a rigorous single-particle model, is in itself of high interest. The present results agree with the Migdal theory calculations of Bauer *et al.* [25] and Ring *et al.* [26] and show again the validity of these calculations. Moreover the knowledge of the $M1$- and $E2$-interaction allows to determine from measured γ-decay data the wave functions of the states quantitatively [22]. The structure of the high-spin one-particle one-hole states and their γ-decays are well understood; all the states of spin 11 and higher are of just one pure configuration.

High-spin two-particle two-hole states in ^{208}Pb have been found for the first time. Spins and parities could not be determined experimentally so far. The first two-particle two-hole shell model calculations with a realistic interaction are not yet precise enough to identify the levels. Only the octupole excitation could be assigned due to its characteristic feature [17]. However, the interaction can be adjusted to the known one-particle one-hole states and will then have much better predictive power. Also new experiments are planned, that should give more detailed data with more efficient detector systems and better beams.

This work was supported by The Polish Scientific Committee Grant No. 2P03B-074-18. One of us (KHM) acknowledges support of the Polish Science Foundation.

References

1. G.H. Herling, T.T.S. Kuo, Nucl. Phys. A **181**, 113 (1970), T.T.S. Kuo, G.H. Herling, US Naval Research Laboratory Report Nr. 2258, 1971 (unpublished).
2. E.K. Warburton, B.A. Brown, Phys. Rev. C **43**, 603 (1991).
3. P. Grabmayr, G. Mairle, U. Schmidt-Rohr, Physikalische Blaetter **55**, Nr. 4, 35 (1999).
4. L. Coraggio, A. Covello, A. Gargano, N. Itaco, T.T.S. Kuo, Phys. Rev. C **60**, 064306 (1999).
5. A. Brown, private communication, 1998.
6. A. Hosaka, K.I. Kuobo, H. Toki, Nucl. Phys. A **444**, 76 (1985).
7. R. Broda, C.T. Zhang, P. Kleinheinz, R. Menegazzo, K.H. Maier, H. Grawe, M. Scgramm, R. Schubart, M. Lach, S. Hofmann, Phys. Rev. C **49**, R575 (1994).
8. W. Królas *Deep-inelastic collisions studied by discrete gamma ray spectroscopy*, Ph.D. Thesis - Institute of Nuclear Physics Report No 1738/PL 1996.
9. M. Schramm, H. Grawe, J. Heese, H. Kluge, K.H. Maier, R. Schubart, R. Broda, J. Grebosz, W. Krolas, A. Maj, J. Blomqvist, Z. Phys. A **344**, 363 (1993).
10. R. Broda, J. Wrzesinski, T. Pawlat, B. Fornal, Z. Grabowski, D. Bazzacco, S. Lunardi, C. Rossi-Alvarez, G. de Amngelis, A. Gadea, K.H. Maier, *Proceedings of the Conference on Nuclear Structure at the Limits, Argonne, Illinois, July 1996*, ANL/Phy-97/1 p. 276.
11. K.H. Maier, Acta Phys. Pol. B **28**, 277 (1997).
12. J. Eberth, *Proceedings of the Conference on Physics from Large gamma-Detector Arrays, August 2-6, 1994, Berkeley, Ca., USA*, vol. II, LBL-356
13. V. Metag, D. Habs, K. Helmer, V. v. Helmdt, H.W. Heyng, B. Kolb, D. Pelte, D. Schwalm, *Lect. Notes Phys.*, Vol. **178** (Springer Verlag, Berlin) ISBN 3-540-12001-7.
14. M. Rejmund, K.H. Maier, R. Broda, M. Lach, J. Wrzesinski, J. Agramunt, J. Blomqvist, A. Gadea, J. Gerl, M. Gorska, H. Grawe, M. Kaspar, I. Kozhoukharov, I. Peter, H. Schaffner, R. Schubart, Ch. Schlegel, G. Stengel, S. Wan, H.J. Wollersheim, Z. Phys. **359**, 243 (1997).
15. M. Rejmund, K.H. Maier, R. Broda, B. Fornal, M. Lach, J. Wrzesinski, J. Blomqvist, A. Gadea, J. Gerl, M. Gorska, H. Grawe, M. Kaspar, H. Schaffner, Ch. Schlegel, R. Schubart, H.J. Wollersheim, Eur. Phys. J. A **1**, 261 (1998).
16. D.C. Radford, Nucl. Instrum. Methods A **361**, 297 (1995).
17. M. Rejmund, K.H. Maier, R. Broda, B. Fornal, M. Lach, J. Wrzesiński, J. Blomqvist, A. Gadea, J. Gerl, M. Górska, H. Grawe, M. Kaspar, H. Schaffner, Ch. Schlegel, R. Schubart, H.J. Wollersheim, Eur. Phys. J. A **8**, 161 (2000).
18. A.D. Bacher, G.T. Emery, W.P. Jones, D.W. Miller, G.S. Adams, F. Petrovich, W.G. Love, Phys. Lett. B **97**, 58 (1980).
19. J. Lichtenstadt, J. Heisenberg, C.N. Papanicolas, C.P. Sargent, A.N. Courtemanche, J.S. McCarthy, Phys. Rev. Lett. **40**, 1127 (1978).

20. J.P. Connelly, D.J. de Angelis, J.H. Heisenberg, F.W. Hersman, W. Kim, M. Leuschner, T.E. Milliman, J. Wise, Phys. Rev. C **45**, 2711 (1992).
21. A.D. Bacher in *Polarization Phenomena* in *Nucl. Phys.*, **5** *AIP Conf. Proc.*, edited by G.G. Ohlsen, R.E. Brown, N. Jarmie, W.W. McNaughton, G.M. Hale, Vol. **69** (1980), p. 220.
22. M. Rejmund, M. Schramm, K.H. Maier, Phys. Rev. C **59**, 2520 (1999).
23. N. Roy, K.H. Maier, A. Aprahamian, J.A. Becker, D.J. Decman, E.A. Henry, L.G. Mann, R.A. Meyer, W. Stöffl, G.L. Struble, Phys. Lett. B **221**, 6 (1989).
24. M.J. Martin, Nucl. Data Sheets **63**, 754 (1991); 220 (1980).
25. R. Bauer, J. Speth, V. Klemt, P. Ring, E. Werner, T. Yamazaki, Nucl. Phys. A **209**, 535 (1973).
26. P. Ring, R. Bauer,, J. Speth, Nucl. Phys. A **206**, 97 (1973).
27. L. Rydström, J. Blomqvist, R.J. Liotta, C. Pomar, Nucl. Phys. A **512**, 217 (1990).
28. J.B. McGrory, T.T.S. Kuo, Nucl. Phys. A **247**, 283 (1975).
29. T.T.C. Kuo, G.E. Brown, Nucl. Phys. **85**, 40 (1966).